OXFORD

molecular human reproduction

Molecular Human Reproduction, 2025, **31(1)**, gaaf001

https://doi.org/10.1093/molehr/gaaf001
Advance Access Publication Date: January 25, 2025
Original Research

Pro-cumulin addition in a biphasic *in vitro* oocyte maturation system modulates human oocyte and cumulus cell transcriptomes

Berta Cava-Cami [1,*], Antonio Galvao [2,3,4], Heidi Van Ranst [1], William A. Stocker [5], Craig A. Harrison [5], Johan Smitz [1], Michel De Vos [1,6], Gavin Kelsey [3,7,8], and Ellen Anckaert [1]

[1]Follicle Biology Laboratory, Research Group Genetics, Reproduction and Development, Vrije Universiteit Brussel (VUB), Brussels, Belgium
[2]Institute of Animal Reproduction and Food Research, Polish Academy of Science, Olsztyn, Poland
[3]Babraham Institute, Epigenetics Programme, Cambridge, UK
[4]Department of Comparative Biomedical Sciences, Royal Veterinary College, London, UK
[5]Department of Physiology, Monash Biomedicine Discovery Institute, Monash University, Clayton, VIC, Australia
[6]BrusselsIVF, Universitair Ziekenhuis Brussel, Brussels, Belgium
[7]Centre for Trophoblast Research, University of Cambridge, Cambridge, UK
[8]Wellcome-MRC Institute of Metabolic Science-Metabolic Research Laboratories, Cambridge, UK

*Correspondence address. Follicle Biology Laboratory, Research Group Genetics, Reproduction and Development, Vrije Universiteit Brussel (VUB), Laarbeeklaan 103, Building K, 1090 Brussels, Belgium. E-mail: bertacava26@gmail.com https://orcid.org/0000-0002-8547-0532

ABSTRACT

Biphasic IVM can be offered as a patient-friendly alternative to conventional ovarian stimulation in IVF patients predicted to be hyper-responsive to ovarian stimulation. However, cumulative live birth rates after IVM per cycle are lower than after conventional ovarian stimulation for IVF. In different animal species, supplementation of IVM media with oocyte-secreted factors (OSFs) improves oocyte developmental competence through the expression of pro-ovulatory genes in cumulus cells. Whether the addition of OSFs in human biphasic IVM culture impacts the transcriptome of oocytes and cumulus cells retrieved from small antral follicles in minimally stimulated non-hCG-triggered IVM cycles remains to be elucidated. To answer this, human cumulus–oocyte complexes (COCs) that were fully surrounded by cumulus cells or partially denuded at the time of retrieval were cultured in a biphasic IVM system either without or with the addition of pro-cumulin, a GDF9:BMP15 heterodimer. Oocytes and their accompanying cumulus cells were collected separately, and single-cell RNA-seq libraries were generated. The transcriptomic profile of cumulus cells revealed that pro-cumulin upregulated the expression of genes involved in cumulus cell expansion and proliferation while downregulating steroidogenesis, luteinization, and apoptosis pathways. Moreover, pro-cumulin modulated the immature oocyte transcriptome during the pre-maturation step, including regulating translation, apoptosis, and mitochondria remodeling pathways in the growing germinal vesicle oocytes. The addition of pro-cumulin also restored the transcriptomic profile of matured metaphase II oocytes that were partially denuded at collection. These results suggest that cumulus cell and oocyte transcriptome regulation by pro-cumulin may increase the number of developmentally competent oocytes after biphasic IVM treatment. Future studies should assess the effects of pro-cumulin addition in human biphasic IVM at the proteomic level and the embryological outcomes, particularly its potential to enhance outcomes of oocytes that are partially denuded at COC collection.

Keywords: biphasic IVM / oocyte / pre-maturation / oocyte-secreted factors (OSFs) / cumulus cells / RNA-seq / single-cell transcriptomics

Introduction

IVM is an assisted reproductive technology designed to produce mature oocytes through the culture of immature cumulus–oocyte complexes (COCs) aspirated from unstimulated small- and medium-sized antral follicles. Administration of exogenous gonadotropins is kept to a minimum or even absent and there is no exogenous ovulation trigger. As a result, IVM can be offered as a mild alternative to conventional ovarian stimulation in polycystic ovary syndrome (PCOS) patients who are at increased risk of hormone-related side effects (De Vos *et al.*, 2021; Gilchrist and Smitz, 2023; Marchante *et al.*, 2024). Moreover, IVM is a fertility preservation option when conventional ovarian stimulation is not possible, e.g. due to urgent cancer treatment. Although still considered experimental, IVM of oocytes derived from ovarian tissue (OTO-IVM) during processing for ovarian tissue cryopreservation is also emerging as an additional source of mature oocytes (Segers *et al.*, 2015; Cadenas *et al.*, 2023; Nogueira *et al.*, 2023). However, the cumulative live birth rate in women with PCOS is lower after IVM than after conventional IVF (Zheng *et al.*, 2022). One of the main reasons for the reduced quality of IVM oocytes

Received: May 31, 2024. **Revised:** December 15, 2024. **Editorial decision:** January 17, 2025.

retrieved from small antral follicles is the loss of synchronization between nuclear and cytoplasmic maturation *in vitro*.

After decades of extensive research in animal models designed to improve oocyte competence, the biphasic IVM system, termed capacitation (CAPA)-IVM, has been introduced (Luciano *et al.*, 2011; Romero *et al.*, 2016; Zhang *et al.*, 2017; Zhao *et al.*, 2020a). In CAPA-IVM, the natural meiosis-inhibiting peptide, C-type natriuretic peptide (CNP), is added during the pre-maturation (CAPA) step. CNP keeps the oocyte under meiotic arrest by maintaining high oocyte cAMP levels, therefore enhancing oocyte cytoplasmic maturation, before triggering nuclear maturation with FSH and amphiregulin in the IVM step. CAPA-IVM improves the number of matured oocytes and good-quality embryos per cycle compared to standard IVM in women with PCOS (Vuong *et al.*, 2020b). Moreover, CAPA-IVM safety studies have been done in human blastocysts and children born from the technology (Saenz-de-Juano *et al.*, 2019; Nguyen *et al.*, 2022; Saucedo-Cuevas *et al.*, 2024). However, a large randomized controlled trial revealed that cumulative live birth rates were still 18.6% lower when compared to conventional IVF, which reflects the need to improve the biphasic IVM system (Vuong *et al.*, 2020a).

The crosstalk between the oocyte and its surrounding cumulus cells (CCs) is essential for proper oocyte maturation (Wigglesworth *et al.*, 2013). Through oocyte-secreted factors (OSFs), the oocyte orchestrates CC functionality and phenotype, which in turn improves the maturation and developmental competence of the oocyte (Diaz *et al.*, 2007; Stocco *et al.*, 2017). Two widely recognized OSFs are growth differentiation factor 9 (GDF9) and bone morphogenetic protein 15 (BMP15), which form homodimers and/or heterodimers (GDF9:BMP15) (Peng *et al.*, 2013; Mottershead *et al.*, 2015). As crucial paracrine regulators of ovarian function and fertility, OSFs bind their receptors (BMP receptor type II, BMP receptor type IB, and TGF-βRI) on surrounding CCs to activate the transforming growth factor-beta (TGF-β) signaling pathway. Previous studies in different species including porcine, bovine, and mice have shown that the addition of OSFs during monophasic IVM does not affect the maturation rate of the oocytes but modulates CC functionality, which in turn improves embryo development (Hussein *et al.*, 2006; Yeo *et al.*, 2008; Sudiman *et al.*, 2014; Sugimura *et al.*, 2015). Moreover, the addition of a GDF9:BMP15 heterodimer, termed pro-cumulin, strongly promotes extracellular matrix (ECM) formation and expression of CC ovulatory cascade genes when compared to using individual homodimers or their combination (Peng *et al.*, 2013). Previous studies in human granulosa cell (GC) lines (COV434, KGN) confirmed the activation of the SMAD signaling pathway by pro-cumulin, stimulating the expansion, proliferation, and oocyte-regulated differentiation of GCs (Zhang *et al.*, 2000; Spicer *et al.*, 2008). A recent study using pro-cumulin in a biphasic mouse IVM model showed improved CC expansion consistent with an increase in transcripts related to CC ovulatory cascade, more closely resembling the *in vivo* matured COC (Akin *et al.*, 2022). To date, there is only one study testing the *in vitro* addition of OSF to human oocytes, in which denuded immature oocytes after conventional IVF (rescue-IVM) were co-cultured with GCs and GDF9, showing a beneficial effect on blastocyst viability (Chatroudi *et al.*, 2019).

The effects of adding OSFs to biphasic IVM culture media on the transcriptome of human COC retrieved from small antral follicles in minimally stimulated IVM cycles is currently unknown. We therefore set out to assess the effects when adding pro-cumulin during the pre-IVM step only or in both pre-IVM and IVM steps. Additionally, when performing ovarian retrieval in non-hCG primed IVM cycles, a percentage of the retrieved COCs consist of partially denuded oocytes that have a low competence after IVM presumably due to the reduced bidirectional communication between CCs and the oocyte. Previous unpublished data from our laboratory on human CAPA-IVM revealed that more than 20% of oocytes are partially denuded at retrieval, yielding lower embryonic outcomes compared to the fully surrounded counterparts (5% vs 18% Day 5 good-quality blastocyst, respectively). Consequently, we also assessed the potential effects of OSFs in restoring the transcriptome of partially denuded oocytes.

Materials and methods

Ethical approval

This study was approved by the local ethics committee for human clinical studies of the University Hospital UZ Brussel of the Vrije Universiteit Brussel (Study code: BUN/143201630723). Written informed consent was obtained from all oocyte donors before inclusion in the study. The consent form included details on the donation of immature COCs to improve and assess the efficacy of IVM in the presence of OSFs.

Preparation of OSFs

The recombinant human pro-cumulin used in this study was produced and purified at the Department of Physiology, Monash Biomedicine Discovery Institute, as previously described (Stocker *et al.*, 2020). Briefly, HEK-293T cells were transfected with plasmids for both GDF9 and BMP15 using polyethylenimine-MAX (Polysciences, Warrington, PA, USA). Pro-cumulin was then purified from the conditioned medium via cobalt-based IMAC (Thermo Fisher Scientific, Waltham, MA, USA), followed by dialysis against PBS. Purified pro-cumulin was stored in Protein LoBind tubes (Eppendorf, Hamburg, Germany) at −80°C. The pro-cumulin dose used in this study was 20 ng/ml and was based on previous work from Mottershead *et al.* (2015).

Patient characteristics and study design

To prospectively evaluate the impact of pro-cumulin addition to CAPA-IVM media on COC transcriptome and oocyte maturation, a total of 14 oocyte donors with a high functional ovarian reserve participated in this study from July 2020 until July 2021 at the UZ Brussels University Hospital. Inclusion criteria were age below 37 years, more than 30 antral follicles on a baseline ultrasound scan and serum anti-Müllerian hormone (AMH) above 2 ng/ml (Cobas 8000, Roche Diagnostics, Basel, Switzerland). Three of the oocyte donors underwent two IVM cycles, resulting in a total of 17 IVM cycles. In nine of these cycles, all the aspirated COCs were donated for research. In eight cycles, the oocyte donors were patients who underwent IVM and donated one-third of the aspirated COCs. In donors who contributed twice, follicle aspirates from one of the cycles were allocated to experiment 1 and the second cycle aspirates were allocated to experiment 2. The oocyte donors received highly purified menotropin (HP-hMG) for 1–3 days. Ovarian retrieval was scheduled 42–46 h after the last HP-hMG injection and was performed using a 17-gauge single-lumen needle (Cook Medical, K-OPS-1230-VUB, Limerick, Ireland) at a pressure of −70 mmHg. On the day of oocyte retrieval, the aspirates from follicles smaller than 9 mm were pooled, and the retrieved COCs were randomly allocated to the control arm of the study (CAPA-IVM), or the two experimental conditions of the study: CAPA (+pro-cumulin)-IVM and CAPA (+pro-cumulin)-IVM (+pro-cumulin) (Fig. 1).

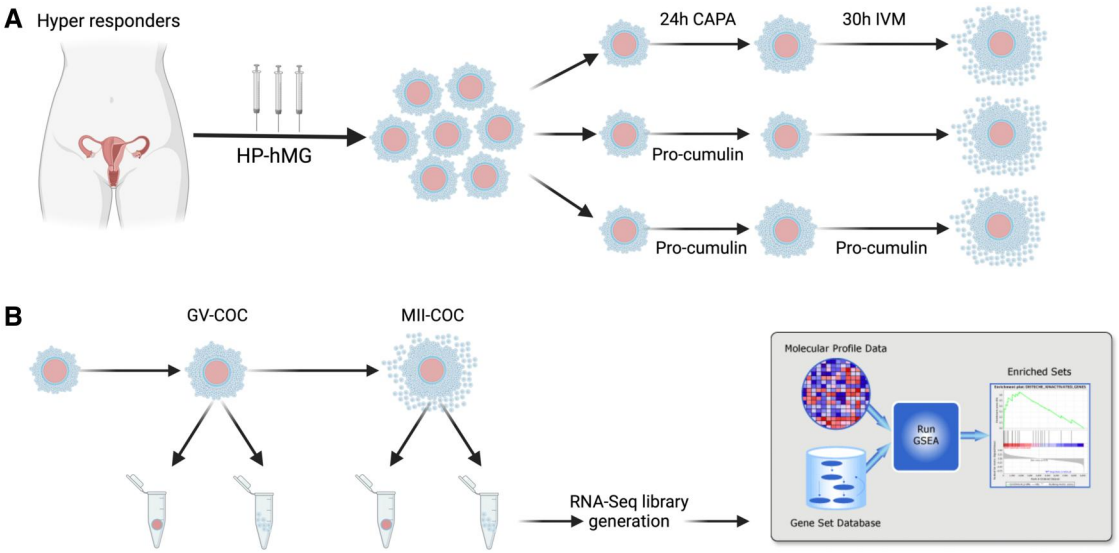

Figure 1. Graphical study design. (**A**) A total of 14 hyper-responder donors were included in the study. Women received two to three HP-hMG injections without ovulatory stimulus before oocyte retrieval. Sibling oocytes were distributed among the study conditions. (**B**) Single oocytes and cumulus cells from individual COCs were collected for library generation. GSEA analysis was performed on differentially expressed genes after DESeq analysis. HP-hMG, highly purified menotropin; COCs, cumulus–oocyte complexes; GSEA, Gene Set Enrichment Analysis.

Collection of COCs and culture conditions

Follicular aspirates were collected in Ferticult Flushing (FertiPro; Beernem, Belgium) media at a final concentration of 25 nM CNP (Peptide Institute, Japan) and 10 nM estradiol (Sigma; Schnelldorf, Germany) and filtered through a cell strainer (70 µm mesh size BD Biosciences Falcon™ Ref 352350). COCs found in the search media (25 nM CNP, 10 nM estradiol, 10 mg/ml human serum albumin (HSA) (Vitrolife, Gothenburg, Sweden; ref: 10064)) were divided into three different categories: (i) fully surrounded COC with at least three to four tightly compact layers of CCs fully surrounding the oocyte; (ii) partially denuded COC when incomplete corona radiata was surrounding the oocyte; and (iii) completely denuded and degenerated oocytes where no CCs were surrounding the oocytes, which were not used for this study. COCs were washed in a 4-well dish (Nunc, ThermoFisher Scientific; ref: 178930) in CAPA medium (Medicult IVM medium; Origio, Denmark) supplemented with 1 mIU/ml rFSH, 5 ng/ml insulin (Roche ref: 11376497001), 10 nM estradiol, 10 mg/ml HSA, and 25 nM CNP. COCs were transferred to a 60-mm dish (ThermoFisher ref: 150270) and individually cultured in 20 µl CAPA medium under mineral oil for 24 h at 37°C, 6% carbon dioxide in air. After 24 h in CAPA medium, COCs were washed in a 4-well dish in IVM medium (Medicult IVM medium supplemented with 100 mIU/ml rFSH, 5 ng/ml insulin, 10 nM estradiol, 10 mg/ml HSA). COCs were transferred to a 60-mm dish and individually cultured in 20 µl pre-equilibrated IVM medium for 30 h at the same incubation conditions. To avoid patient-related effects, sibling COCs were randomly distributed among the two arms of the study to assess the pro-cumulin effect at the germinal vesicle (GV) stage and among the three arms of the study when analyzing metaphase II (MII) and CC-MII transcriptome.

Experiment 1 (7 IVM cycles)

For CC-GV and GV collection: after 24 h CAPA culture, individual COCs were mechanically denuded in HEPES-buffered media containing 100 µM IBMX. Oocytes were scored as GV-oocytes when a visible GV was seen under the stereomicroscope. To assess the proportion of meiosis arrest, the ratio of GV-arrested oocytes versus the total number of oocytes denuded after the CAPA step was calculated. CC-free GV-oocytes were individually collected in 2.5 µl RLT-Buffer (Qiagen, Hilden, Germany) in 0.5 ml Protein LoBind tubes (Eppendorf ref: 022431064) and immediately snap-frozen in liquid nitrogen. A minimum of 50 CCs from each GV were collected in 4 µl of HEPES media and transferred to 0.5 ml Protein LoBind tubes containing 4 µl RLT-Buffer.

Number of samples for experiment 1: a total of 59 GVs were collected (31 GV-Control and 28 GV-Pro-cumulin). Two CC samples per patient were processed for each condition: 14 CC-GV-Control and 14 CC-GV-Pro-cumulin (Fig. 2A).

Experiment 2 (10 IVM cycles)

For CC-MII and MII collection: after 24 h CAPA followed by 30 h IVM, individual COCs were denuded with hyaluronidase (CooperSurgical, Trumbull, VT, USA; ref: 16125000) and washed three times in HEPES media. After denuding, the oocytes were classified into GV, metaphase I (MI), and MII, when a GV was visible in the cytoplasm, when no GV was present, and when no GV and the polar body was extruded, respectively. To assess the percentage of maturation after CAPA-IVM, the total number of matured oocytes was divided by the number of denuded oocytes per patient and condition. CC-free MII oocytes were snap-frozen in 2.5 µl RLT-Buffer in 0.5 ml Protein LoBind tubes. Four microliters of HEPES media containing at least 50 CCs from MII oocytes were snap-frozen in 4 µl RLT-Buffer in 0.5 ml Protein LoBind tubes.

Number of samples for experiment 2.1: a total of 72 MII from fully surrounded oocytes at collection, 24 MII-Control, 24 MII-CAPA-Pro-cumulin, and 24 MII-CAPAIVM-Pro-cumulin were collected. One CC sample per patient was processed for each condition: 10 CC-MII Control, 10 CC-MII CAPA-Pro-cumulin, and 10 CC-MII CAPAIVM-Pro-cumulin were collected (Fig. 2B).

Number of samples for experiment 2.2: a total of 21 MII oocytes from partially denuded (termed DO) COCs were collected from the three arms of the study: 8 DO-MII-Control CAPA-IVM, 8 DO-MII-CAPA-Pro-cumulin, and 5 DO-MII-CAPAIVM; these were compared with matured oocytes from fully surrounded COCs at collection (24 MII CAPA-IVM). Due to the lower number of CCs in partially denuded oocytes, CCs were not collected (Fig. 2C).

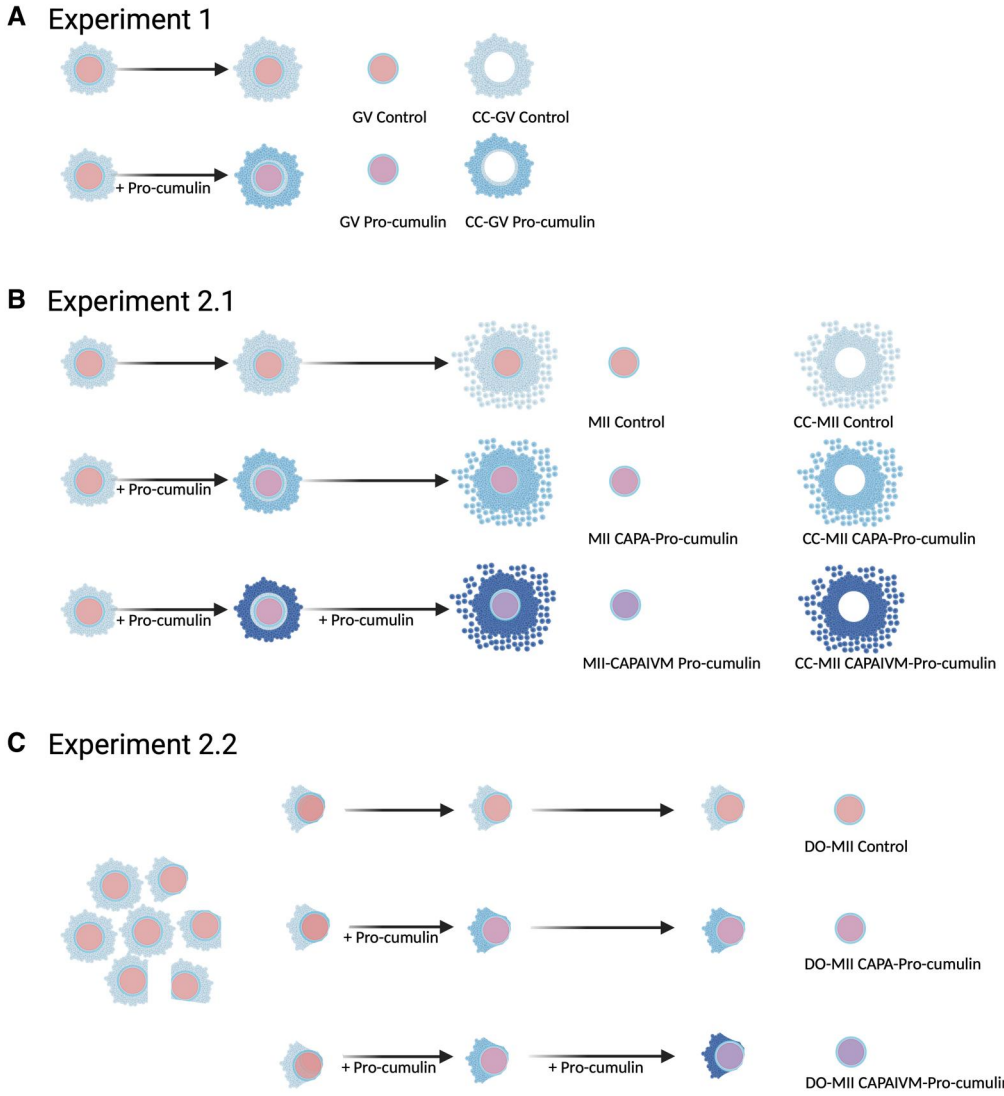

Figure 2. Graphical study design summarizing the various experimental treatments. (**A**) Experiment 1: GV-Control and GV-Pro-cumulin oocytes collected after 24 h CAPA and their corresponding CCs. (**B**) Experiment 2.1: MII-Control and MII-Pro-cumulin oocytes IVM and their corresponding CCs after 24 h CAPA followed by 30 h. (**C**) Experiment 2.2: Partially denuded oocytes retrieved at collection were cultured in the same conditions as experiment 2.1. The transcriptome profile of the partially denuded oocytes was compared to MII-Control, from fully surrounded COCs. GV, germinal vesicle; CCs, cumulus cells; MII, metaphase II; COCs, cumulus–oocyte complexes; DO, partially denuded oocyte; CAPA, capacitation.

Sample processing: RNA extraction and single-cell RNA-seq library generation

For mRNA extraction, individual oocytes or bulk CCs from one COC were used. RNA and DNA extraction from single oocytes and CCs was performed simultaneously using oligo-dT magnetic beads (Dynabeads, MyOne Streptavidin C1, Life Technologies, Carlsbad, CA, USA) as RNA binds to beads. The supernatant containing DNA was washed and stored for future use. RNA from individual oocytes and CCs was isolated following the Genome & Transcriptome protocol (Angermueller *et al.*, 2016). Briefly, RNA was eluted from the beads, lysated, and converted into cDNA by the enzyme Superscript II and oligo-dT primers.

cDNA was amplified using KAPA HiFi HotStart ReadyMix (Roche) and assessed for integrity using a High Sensitivity DNA Assay Kit of the Bioanalyzer® 2100 system (Agilent Technologies, Inc., Santa Clara, CA, USA). The cDNA was stored at −20°C until libraries were generated. RNA library generation for single oocytes was constructed in one single batch. mRNA library preparation was carried out using the Nexetra XT DNA library preparation Kit No. FC-131-1024 (Illumina, Inc., San Diego, CA, USA). RNA sequencing was conducted on the NextSeq500 HighOutput 75-bp Single End with a sequence depth of ∼3 million reads for oocytes and ∼6 million reads for CCs (Illumina, Inc.).

Raw data priming and bioinformatics analysis

For library trimming and mapping, Trim Galore v0.6.6 was used with default parameters on raw FasQC sequence files. Mapping of the RNA-seq data was done with Hisat v2.0.5 against the human Hs38 genome, as guided by known splice sites taken from Ensemble v68. Mapped RNA-seq reads were quantified and analyzed using SeqMonk version v1.48.0 (http://www.bioinformatics.babraham.ac.uk/projects/seqmonk/).

Differential expression analysis was performed using DESeq2 implemented in SeqMonk. Significantly differentially expressed genes (DEGs) were considered for false discovery rate (FDR) <0.05 and a $|\log_2 FC|>1$ for bulk CCs and FDR < 0.1 and a $|\log_2 FC|>0.5$ for single-cell oocytes.

Gene ontology analysis and KEGG pathways

Gene set enrichment analysis (GSEA) was performed using the 'investigate gene sets' function on the website of the Molecular Signature Database (http://www.gsea-msigdb.org/gsea/msigdb/annotate.jsp). We used all DEGs as input, then differentiated between the up- and down-regulated genes and investigated the Hallmark library and all gene ontology (GO) processes to generate charts showing activated and inhibited pathways. Heatmaps were generated with the WishartLab heat mapper tool. When gene enrichment analysis did not cluster genes into pathways, we investigated gene functionality using the 'Reactome' database.

Results

Study population and collected samples

The demographic characteristics of the donors are shown in Table 1. A total of 186 COCs were collected for this study. Mean (± SEM) age was 28.4 ± 4.0 years, BMI was 25.5±4.4 kg/m^2, AMH was 8.6 ± 5.1 ng/ml and the antral follicle count was 41±15. The mean total HP-hMG dose administered to the donors was 458±103 IU. The number of COCs recovered per donor was 22.9 ± 9.7. All donors were confirmed to be negative for hepatitis B, C, COVID-19, and HIV.

CAPA-IVM outcomes

We found no differences in GV meiotic arrest rates: 31 out of 32 oocytes and 28 out of 31 were at the GV-stage after the CAPA step with or without pro-cumulin, respectively. Hence, both control CAPA oocytes and pro-cumulin treated oocytes were maintained in meiotic arrest after 24 h culture.

After CAPA-IVM, there were no differences in maturation rate among the three different culture conditions (77%, 75%, 79% respectively) nor in oocyte diameter (Supplementary Fig. S1).

Pro-cumulin modulates gene expression in growing GV oocytes

A total of 59 GV oocytes were collected and processed for single-cell library generation. Out of these, 30 GV-Control oocytes and 25 GV-Pro-cumulin oocytes passed the quality control as described in the raw data priming section (Supplementary Fig. S1).

After running DESeq with a cut-off value of $|\log_2 FC$ change$|>0.5$ and *P*-value 0.1, a total of 248 DEGs were identified in GV oocytes upon pro-cumulin treatment during the CAPA step (Fig. 3A). Of the 248 DEGs, 75 genes were upregulated and 173 downregulated (Supplementary Tables S1 and S2). GO analysis for downregulated genes showed significantly enriched pathways (FDR>0.05) for response to stress and DNA damage response among others (Fig. 3B–D). Moreover, pro-cumulin downregulated the expression of genes related to transcription and translation pathways in GV oocytes (Fig. 3B and E). Pro-cumulin also downregulated mitochondria-related genes involved in biogenesis and organelle remodeling (Fig. 3B and F) and transcripts related to zinc-finger proteins, nucleotide repair, and oxidative phosphorylation (*ZNF84, ZNF561, ZNF30, POLTB2, TAF2, MRPL33*) (Fig. 3B and G). Previous studies reported that genes such as *TMEM54*, *ARHGAP*, and *SERPINB* were downregulated in oocytes from PCOS women compared to normo-ovulatory women (Gao *et al.*, 2023). In contrast, *NKD2* was found to be upregulated in oocytes from PCOS patients (Dinh *et al.*, 2019). Our results suggest that pro-cumulin could counteract the dysregulated transcription for the aforementioned genes in GV oocytes from PCOS women (Fig. 3B and G). No clustered pathways were found in Hallmark or GO for the 75 upregulated genes after pro-cumulin treatment. Therefore, the 10 most significant DEGs (all upregulated) with pathway description were assessed by the KEGG source (Table 2).

Among the top 10 upregulated genes, several genes possibly related to meiosis regulation were upregulated in growing GV oocytes upon pro-cumulin addition, such as *EPHA10* and *PPP2R5B*.

Our results also show that pro-cumulin activated the PI3K/Akt pathway in GV oocytes and increased the expression of *IGFBP2*, which encodes an insulin-like growth factor-binding protein, and promotes the expression of *ACTR1B*, which transduces signals from several members of the TGF family such as cytokines, activins, and BMPs. Interestingly, pro-cumulin promotes Glypican 1 (*GPC1*) expression in GV oocytes, which interacts with growth factors such as FGF and TGF-β, WNT, and BMPs (Watson *et al.*, 2012; Pan and Ho, 2021). Moreover, even though we found upregulated *GPC1* in oocytes, *GPC1* mRNA abundance in CCs is considered a potential embryo quality marker (Xiong *et al.*, 2019). *MLLT6* and *SPATC1L* were also found in the top 10 upregulated genes, and are associated with chromosome and centriole-associated proteins, and growth arrest-specific genes *GAS-AS1* and *GAS6*, which play a crucial role during oocyte cytoplasmic maturation and early embryonic development (Kim *et al.*, 2018, 2021) (Table 2).

Finally, in addition to the 10 top upregulated genes, metabolism-related genes were also upregulated upon pro-cumulin treatment in GV oocytes, such as *ABHD12* which is involved in arachidonate production and metabolite transporters, such as *SLC52A*, a riboflavin transporter, *ASPSCR1* which interacts with GLUT4 transporter, and *RPIA* which is involved in pyrimidine metabolism (Supplementary Table S2). Pro-cumulin also increased the expression of *CLTB*, which is involved in the formation of annular gap junctions and WNT signaling.

Thus, pro-cumulin downregulates GV oocyte transcription and mitochondrial pathways which are associated with oocyte competence acquisition. Moreover, pro-cumulin may improve metabolic performance in oocytes from PCOS women, by upregulating the expression of metabolism genes important for nourishing and supporting oocyte growth, while alleviating stress.

Pro-cumulin does not affect fully surrounded MII oocytes, but restores the transcriptome of partially denuded oocytes

A total of 72 MII oocytes were collected and processed for single-cell RNA-seq analysis, from which 70 passed the quality

Table 1. Patient characteristics.

	Mean ± SEM
Age	28.4±4.0
BMI	25.5±4.4
AMH (ng/ml)	8.6±5.1
FSH (IU/l) previous to Menopur treatment	5.8±2.1
Progesterone (μg/l) previous to Menopur treatment	0.2±0.1
Estradiol (ng/l) previous to Menopur treatment	34.1±15.6
LH (IU/l) previous to Menopur treatment	7.8±4.1
Length of stimulation*	2/3*
Dose of stimulation IU (Menopur: highly purified metropin (HP-hMG))	500–650
FSH (IU/l) after Menopur treatment	8.7±1.7
Progesterone (μg/l) after Menopur treatment	0.2±0.1
Estradiol (ng/l) after Menopur treatment	340.6±396.4
LH (IU/l) after Menopur treatment	3.8±2.4
Antral follicle count (AFC)	41±15
COCs recovered per retrieval	22.9±9.7
Fully surrounded COCs	136
Partially denuded COCs	55

* Days.
AMH, anti-Müllerian hormone; COCs, cumulus–oocyte complexes

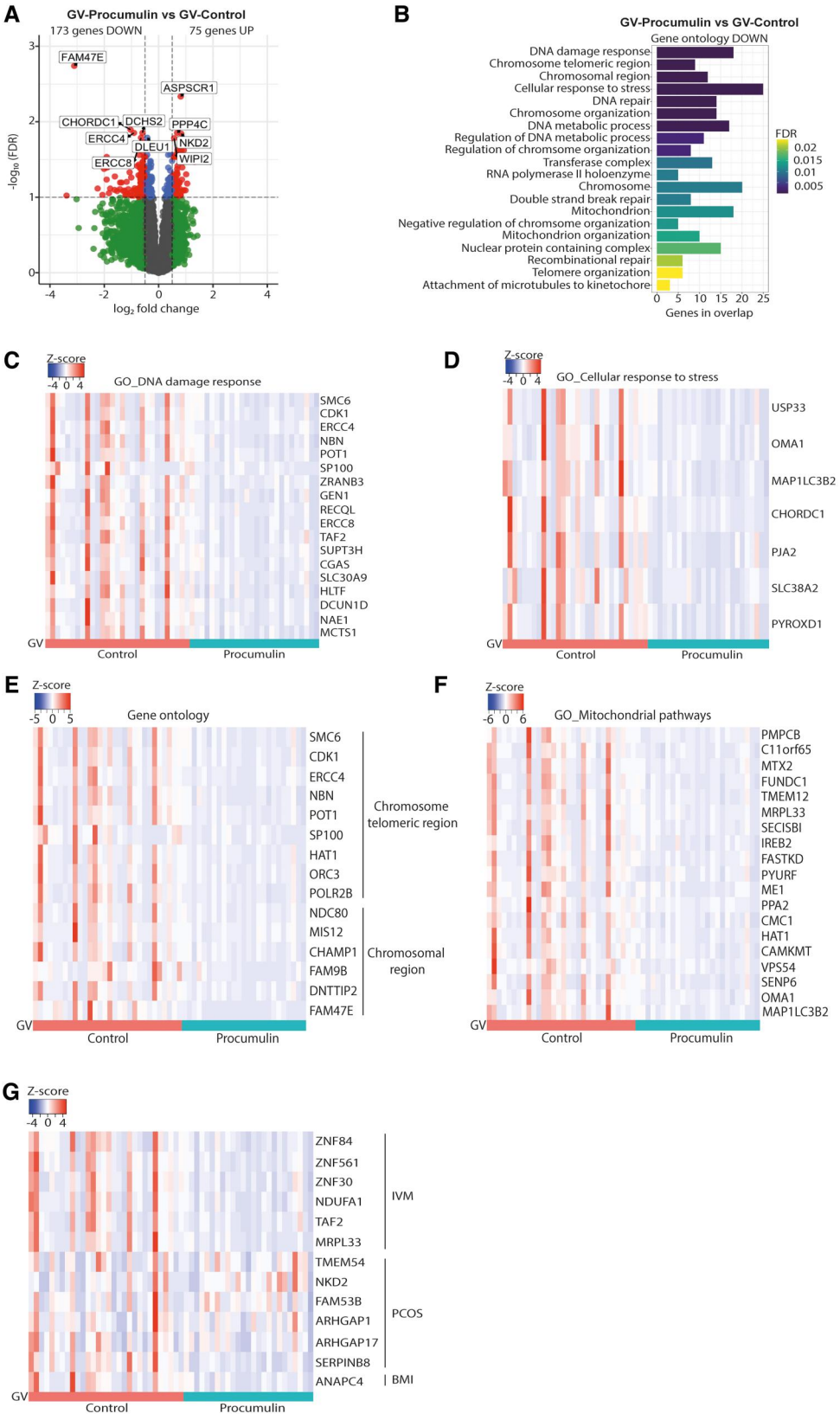

Figure 3. Gene set enrichment analysis (GSEA) of gene expression differences between treatments in GV oocytes. (**A**) Volcano plot of 248 differentially expressed genes identified as being modulated by pro-cumulin in GV oocytes. (**B**) The top 20 gene ontology pathways that are significantly (FDR <0.1) enriched for downregulated genes. (**C–G**) Heatmaps showing supervised clustering of genes involved in the inhibition or activation of gene ontology pathways. GV, germinal vesicle; FDR, false discovery rate.

control. An overall decrease of 23.3% in the total number of transcripts was seen in mature oocytes compared to immature GVs (Fig. 4A).

We therefore investigated first whether the DEGs seen in GV oocytes after pro-cumulin treatment were still expressed in matured oocytes. A total of 222 genes out of 248 DEGs found at the GV stage

Table 2. The 10 most significantly upregulated genes in pro-cumulin-treated germinal vesicle (GV) oocytes compared to the GV control.

Gene symbol	Gene name	FDR	Log2 fold change	Function/pathways
PODXL2	Podocalyxin-like protein 2	0.034	13.243	Cell–cell adhesion: GO:0007155
MLLT6	Protein AF-17	0.065	1.050	Chromosome and associated proteins
EPHA10	Ephrin type-A receptor 10	0.049	1.012	Axon guidance
AMZ1	Archaemetzincin-1	0.081	0.988	Metalloproteases
GPC1	Glypican-1	0.023	0.924	Fibroblast growth factor binding
GAS6-AS1	long noncoding RNA	0.080	0.923	GAS6 antisense RNA1
SPATC1L	Speriolin-like protein	0.034	0.915	Not characterized in oocytes
PPP2R5B	Serine_threonine-protein phosphatase 2A	0.082	0.879	Oocyte meiosis: KEGG_04114; Wnt signaling: KEGG_04310
ENSG00000270792	lncRNA_gene	0.027	0.868	Novel transcript
IGFBP2	Insulin-like growth factor-binding protein 2	0.040	0.867	Glucose metabolism and insulin pathway signaling

FDR, false discovery rate; GO, gene ontology.

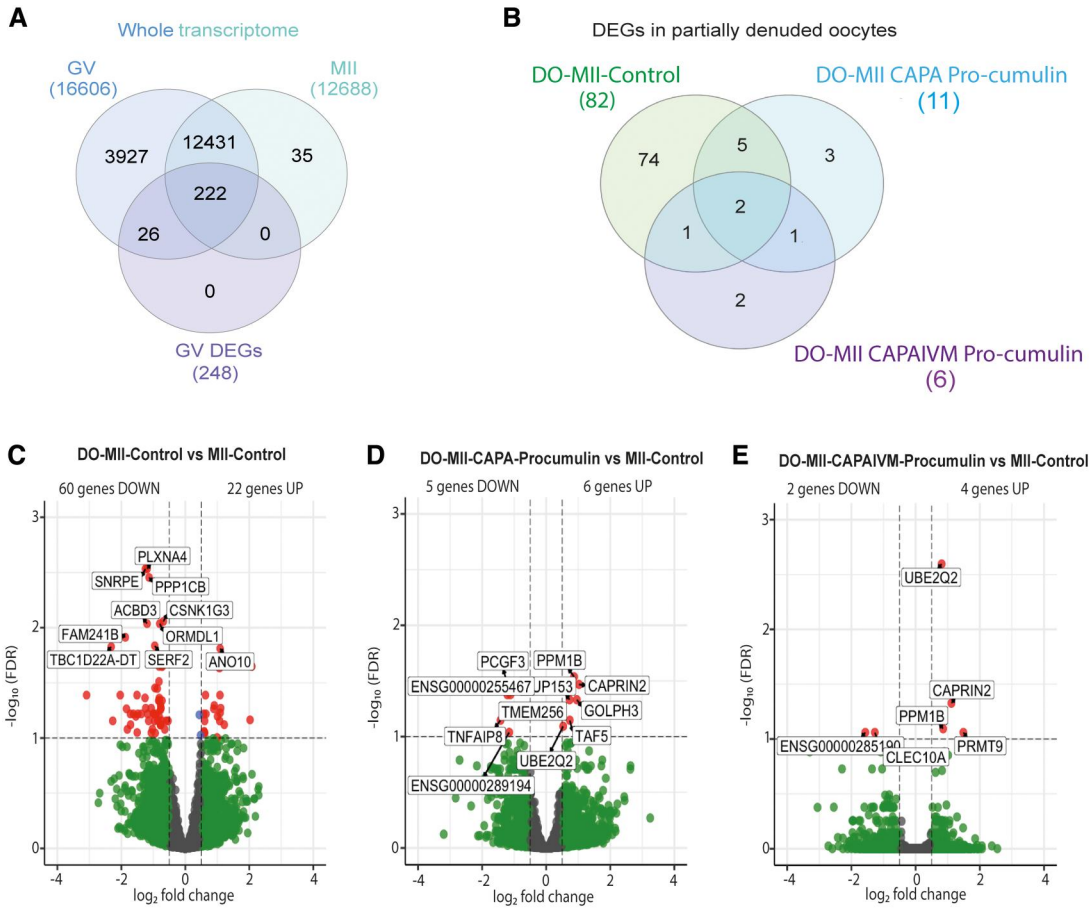

Figure 4. Differentially expressed genes between treatments in MII oocytes. (**A**) Venn diagram displaying the total number of transcripts detected in GV oocytes compared to MII oocytes. A total of 222 DEGs from GVs are still detectable in MII oocytes. (**B**) Venn diagram displaying the common DEGs in partially denuded oocytes among the three treatment conditions. (**C–E**) Volcano plots comparing the transcriptome of fully surrounded MII oocytes to transcripts in DO-MII-CAPA-control, DO-MII-CAPA-Pro-cumulin, and DO-MII-CAPAIVM-Pro-cumulin, respectively. MII, metaphase II; GV, germinal vesicle; DEGs, differentially expressed genes; DO, denuded oocyte; CAPA, capacitation.

upon pro-cumulin treatment were still expressed in MII oocytes (Fig. 4A), suggesting that pro-cumulin could continue affecting oocyte expression for the majority of the genes during the IVM phase.

We next compared the effect of pro-cumulin on the transcriptome of MII oocytes that were fully surrounded at collection. Compared to MII-controls, pro-cumulin-treated MII-CAPA and MII-CAPA IVM oocytes revealed no down-regulated DEGs and one upregulated gene (*CAPRIN*, Supplementary Fig. S2), respectively. However, when comparing the MII oocyte transcriptome from fully versus partially surrounded COCs at collection, named as DO-Control (Denuded Oocyte), a total of 82 DEGs were found (Fig. 4B and C). Partially denuded oocytes had altered expression of genes related to cell cycle and chromatin remodeling (*AVEN*, *LCMT1*), post-translation modifications (*VDAC*, *NUP153*), lipid homeostasis, and mitochondria compared to the fully surrounded counterparts (Supplementary Tables S3 and S4). The lists of the top 10 down- and up-regulated genes in DO-MII-control oocytes are shown in Tables 3 and 4, respectively. Among the top 10

downregulated genes, we found *SAT1* and *RAB13* which are involved in vesicle-mediated transport, and metabolism-related genes such as *ACSM3*, which is involved in beta-oxidation, and to metallothionein (*MT2A*), which is involved in ion and zinc homeostasis and redox metabolism. Among the top 10 upregulated genes, we found *CLK4*. Previous studies correlated the expression of CLK4 in fish embryos with exposure to environmental stress conditions (Whiteley *et al.*, 2021). CLK4 is considered to be a thermosensitive gene, which drives ubiquitination and downstream alternative splicing regulation linked to sex reversal and epigenetic modifications. Another upregulated gene in partially denuded oocytes is *LINC01122*, an uncharacterized long intergenic non-protein coding RNA that has been associated with high BMI and PCOS diagnosis (Brower *et al.*, 2019). Among other upregulated genes in partially denuded oocytes, we found *ANO10*, also known as TMEM16K, which belongs to the anoctamin family of calcium-activated chloride channels, with lipid scramblase activity. Genes related to apoptosis such as *AVEN* were also upregulated.

CAPRIN was upregulated in partially denuded oocytes compared with fully surrounded counterparts, independently of pro-cumulin addition (Fig. 4D and E). However, pro-cumulin treatment in partially denuded COCs largely restored the fully surrounded phenotype in MII oocytes as only 11 and 6 DEGs were found when pro-cumulin was added only during CAPA and during CAPA-IVM, respectively (Fig. 4D and E) (Supplementary Tables S5–S8).

Thus, pro-cumulin modulates the transcriptome in GV oocytes, but does not alter final transcripts present at the MII stage (Supplementary Fig. S2A). However, when oocytes undergo IVM without supportive CCs, alterations in MII transcripts were mitigated by pro-cumulin addition (Supplementary Tables S7 and S8).

Pro-cumulin maintains the CC phenotype and promotes CC expansion

After running DESeq analysis with a cut-off value of $|\log_2$ fold change$|>1$ and *P*-value 0.05, we found 283 DEGs in CC-MII upon pro-cumulin treatment when added in both CAPA and IVM steps, of which 154 were upregulated and 129 were downregulated (Fig. 5A) (Supplementary Tables S9 and S10).

Genes involved in CC expansion and ECM organization were found to be upregulated upon pro-cumulin treatment (Fig. 5B and D–F). GO analysis for upregulated genes showed significant enrichment in pathways related to activated epithelial–mesenchymal transition, apical junction, and metalloproteases pathways (Fig. 5B and D). An increase in CC proliferation by pro-cumulin was reflected by enrichment for pathways involved in mitosis, transcription, and translation (Fig. 5B and E). Moreover, inflammatory responses, IL6–JAK–STAT3 signaling and IL2–STAT5 signaling, and cytokine-based pregnancy biomarkers, were also enriched for upregulated genes (Fig. 5B and F). ECM expansion was observed in all conditions (Supplementary Fig. S3A). Hyaluronan synthase (*HAS2*) and *VERSICAN* (*VCAN*) are genes involved in CC expansion, and their expression has been detected in CC and CC pro-cumulin-treated samples. However, the differences were not significantly different among conditions (FDR > 0.05) (Supplementary Fig. S3B). Pro-cumulin additionally upregulated genes involved in preventing apoptosis (*DDIAS, PDGFRA, GAS5*) and downregulated activators of apoptosis (*DDIT4, PMAIP1, SAT1, TIMP1*, and *SC5D*) (Fig. 5B, C, and G).

Pro-cumulin addition downregulated genes involved in cholesterol homeostasis and lipid metabolism (*STAR, HSD17B7, HSD3B2, CYP51A1*, and MVK), thus reflecting the CC phenotype, as opposed to a mural/luteal GC phenotype and stimulated *SFRP4* gene expression, which are associated with anti-luteinizing effects (Fig. 5C and H). The expression of the luteinizing hormone receptor (LHCGR) was lower in CC upon pro-cumulin treatment. However, the FDR value was higher than the established cut-off for significant differences after DESeq analysis. Specific genes involved in steroidogenesis, listed in the KEGG steroid biosynthesis and steroid hormone pathways, were plotted in the Volcano plot, showing these genes clustering in the downregulated section, and reflecting the overall decreased expression of genes related to steroidogenesis (Supplementary Fig. S3D). Pro-cumulin inactivated the mTOR pathway in CCs (Fig. 5C). Moreover, genes associated with PCOS phenotype in CC were downregulated (*VTN, HSD17B7, CYP11A*) and genes associated with floating GCs compared with CCs surrounding the oocyte were downregulated (*TMEM37, TRIB3*) (Fig. 5I) (Kōks *et al.*, 2010; Khan *et al.*, 2019).

An intermediate transcriptome profile was found in CCs when pro-cumulin was added only during the capacitation step. A total of 49 DEGs were found when compared with control CAPA-IVM MII, where 26 genes were upregulated and 23 downregulated (Supplementary Fig. S2B) (Supplementary Tables S11 and S12). Interestingly, the main pathways downregulated when pro-cumulin was added in both steps, such as steroidogenesis and luteinization, were not downregulated when not adding pro-cumulin from the IVM step (Supplementary Fig. S2). As for pro-cumulin added in both steps, cholesterol biogenesis was the major downregulated pathway, although fewer cholesterol genes were downregulated when compared to CCs which were exposed to pro-cumulin only during the capacitation step (Fig. 5J). A total of 13 DEGs in CCs from MII oocytes were common between pro-cumulin added only during the capacitation step or during both culture steps (Fig. 5J). When we compared CCs from GV oocytes after the CAPA step, we found no differences in the transcriptome between CCs-CAPA Control and CCs-CAPA-pro-cumulin (Supplementary Fig. S2C). The total number of transcripts in CCs did not differ between GV and MII stages. However, 1852 transcripts were specific for CC-GV and 1127 specific for CCs-MII. Of the 283 DEGs found among CC-MII, 266 were also expressed in CC-GVs although pro-cumulin did not affect the expression at the immature stage (Fig. 5K).

Thus, in spite of a major effect of pro-cumulin on CCs transcriptome from matured oocytes, pro-cumulin does not affect the transcriptome in CCs from GV oocytes.

Discussion

Biphasic IVM consists of a pre-maturation step under oocyte meiotic arrest and preserved bidirectional communication between the oocyte and CCs in order to enhance oocyte cytoplasmic maturation prior to nuclear maturation in the IVM step (Gilchrist and Smitz, 2023). Biphasic IVM improves embryological outcomes in PCOS patients when compared to standard monophasic IVM (Vuong *et al.*, 2020b). However, to reduce the remaining efficiency gap between biphasic IVM and conventional IVF (Vuong *et al.*, 2020a), further optimization of IVM culture conditions is required. Previous studies in mice and human IVM reported that culturing the oocytes *in vitro* altered the gene expression profile (Virant-Klun *et al.*, 2013; Llonch *et al.*, 2021; Zhang *et al.*, 2021). In several animal models, supplementation of culture media with paracrine factors naturally secreted by oocytes enhanced the developmental competence of oocytes matured in monophasic IVM. Although not affecting oocyte maturation rates, beneficial effects were achieved in mice, bovine, porcine or ovine in terms

Table 3. The 10 most significantly downregulated genes in partially denuded (DO)-metaphase II (MII) oocytes compared to fully surrounded MII oocytes.

Gene symbol	Description	FDR	Log2 fold change	Pathways
RAB13	RAB13, member RAS oncogene family [Source: HGNC Symbol; Acc: HGNC: 9762]	0.040	−3.087	Tight junctions
TBC1D22A-DT	TBC1D22A divergent transcript [Source: HGNC Symbol; Acc: HGNC: 55388]	0.015	−2.316	Membrane trafficking
ACSM3	Acyl-CoA synthetase medium chain family member 3 [Source: HGNC Symbol; Acc: HGNC: 10522]	0.069	−2.272	Lipid biosynthesis
MT2A	Metallothionein 2A [Source: HGNC Symbol; Acc: HGNC: 7406]	0.040	−2.034	Motor proteins–cytoskeleton
FAM241B	Family with sequence similarity 241 member B [Source: HGNC Symbol; Acc: HGNC: 23519]	0.012	−1.874	Uncharacterized protein – predicted to play a role in lysosome homeostasis
SNTG2	Syntrophin gamma 2 [Source: HGNC Symbol; Acc: HGNC: 13741]	0.054	−1.838	PDZ domain-containing proteins
SAT1	Spermidine/spermine N1-acetyltransferase 1 [Source: HGNC Symbol; Acc: HGNC: 10540]	0.083	−1.812	Transcription factor
LINC02553	Long intergenic non-protein coding RNA 2553 [Source: HGNC Symbol; Acc: HGNC: 53588]	6.92E−4	−1.767	Not characterized
ENSG00000241073	Novel transcript	0.060	−1.720	Not characterized
ENSG00000280320	Novel transcript	0.076	−1.710	Not characterized

FDR, false discovery rate.

Table 4. The 10 most significantly upregulated genes in denuded (DO)-metaphase II (MII) oocytes compared to fully surrounded MII oocytes.

Gene symbol	Gene name	FDR	Log2 fold change	Pathways
ENSG00000287476	lncRNA (Novel Transcript)	0.023	2.08	Not characterized
CLK4	CDC like kinase	0.068	2.024	Splicing-specific kinases
OLFML1	Olfactomedin like 1	0.076	1.22	Embryonic development and tumorigenesis
CAPRIN2	Caprin family member	4.09E−4	1.193	mRNA binding protein
AVEN	Apoptosis and caspase activation inhibitor	0.053	1.11	Cell death regulator
KIAA1328	Uncharacterized protein	0.060	1.088	Protein hinderin
ANO10	Anoctamin-10	0.015	1.088	Induction of cell–cell fusion
LINC01122	Long intergenic non-protein coding RNA 161	0.040	1.084	Topologically associated domains (TADs)
VDAC3	Voltage-dependent anion-selective channel protein 3	0.070	1.077	Mitochondrial calcium ion transport
LCMT1	Leucine carboxyl methyltransferase 1	0.023	1.067	Cyclin A/B1/B2-associated events during G2/M transition

FDR, false discovery rate.

of CC gene expression or blastocyst yield (Su *et al.*, 2004; Hussein *et al.*, 2006; Mottershead *et al.*, 2015; Sutton-McDowall *et al.*, 2015; Akin *et al.*, 2022) and in terms of mice fetal viability (Yeo *et al.*, 2008; Sudiman *et al.*, 2014).

This is the first study which examined the effect of OSF supplementation during human biphasic IVM on CC and the oocyte transcriptomes. Besides its relevance for clinical IVM, the biphasic IVM model allows the study of molecular events endorsing nuclear but also cytoplasmic maturation at two different maturation stages: the GV-stage after the pre-maturation step and the MII stage after IVM.

Our study demonstrated that the addition of a GDF9:BMP15 heterodimer, termed pro-cumulin, during human biphasic IVM preserves the CC transcriptomic profile, thus counteracting the *in vitro* de-differentiation of CC toward the mural GC phenotype. Moreover, pro-cumulin regulates the GV oocyte transcriptome during the pre-maturation step. Pro-cumulin did not modulate the MII transcriptome from fully surrounded COCs during IVM. However, pro-cumulin addition mitigated the transcriptional changes induced by partial oocyte denudation at COC collection (Fig. 6).

RNA-seq data from the current study show that pro-cumulin supplementation during the first (capacitation) step of biphasic IVM modulates the transcriptome in growing GV-oocytes. GO analysis for downregulated genes showed significant enrichment for response to stress pathways. During *in vitro* growth and maturation, the oocytes are exposed to several sources of stress (Von Mengden *et al.*, 2020; Yan *et al.*, 2021). Therefore, downregulated cell-response stress pathways in our study may reflect the beneficial effect of pro-cumulin in reducing culture-induced cellular stress. A decreased DNA damage response, including RNA polymerase II, DSBs, chromosome, and ribosome-related gene transcripts, suggests that gene transcription is downregulated and protein translation is decreased by pro-cumulin, which are known to coincide with surrounded nucleolus (SN) organization and acquisition of meiotic competence (Miyara *et al.*, 2003; Bogolyubova *et al.*, 2023). Moreover, post-transcriptional regulation genes such as *YKT6* and *THOP1*, which are involved in peptide degradation were upregulated, suggesting that pro-cumulin modulates mRNA stability in growing GV oocytes.

Immature oocytes undergo stages of active transcription and translation during their growing phase, especially during the late

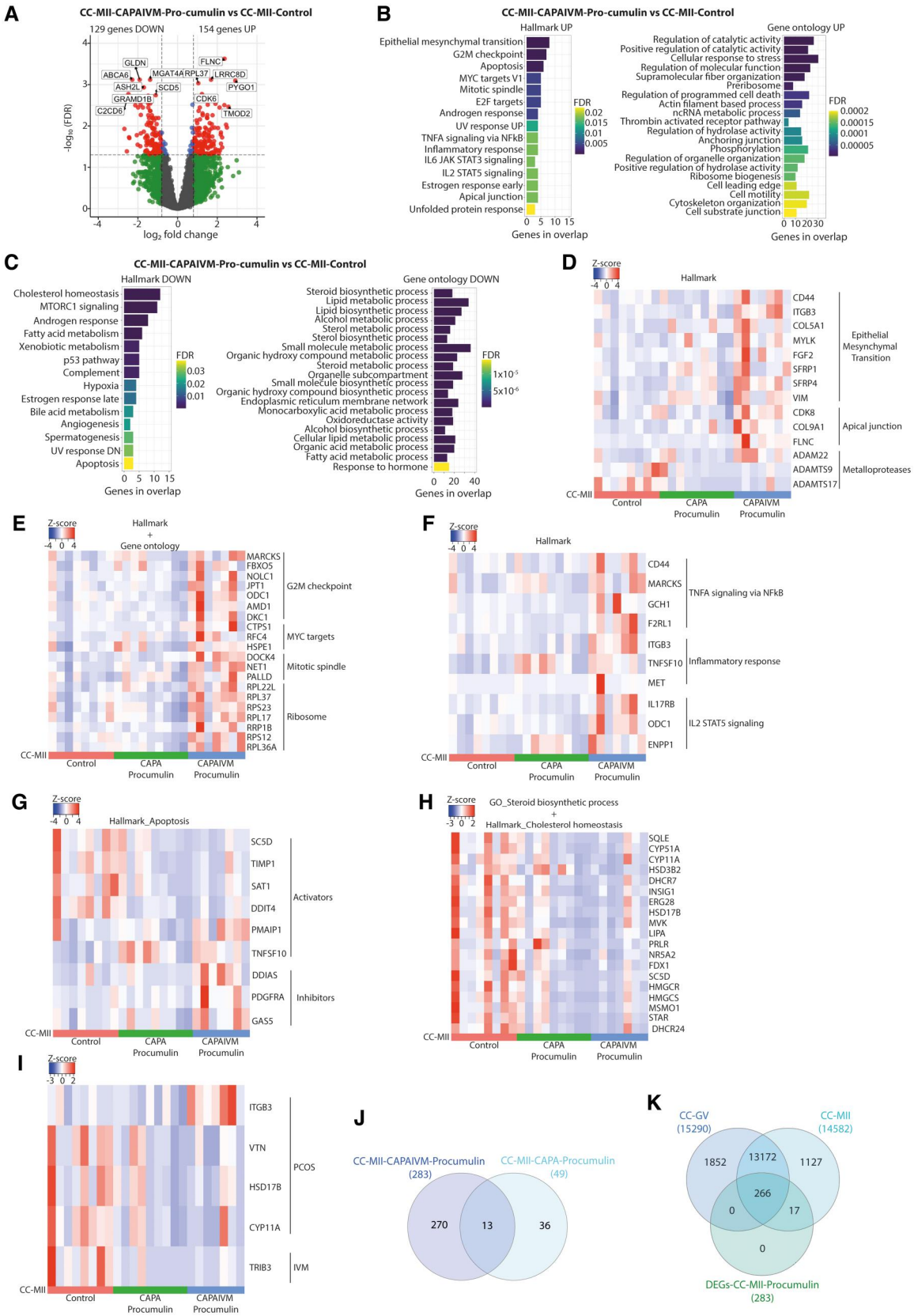

Figure 5. Gene set enrichment analysis (GSEA) of gene expression differences between treatments in cumulus cells. (**A**) Volcano plot of 283 DEGs modulated by pro-cumulin in CC-MII-CAPAIVM pro-cumulin. (**B, C**) Charts show activated and inhibited pathways from Hallmark library and gene ontology (GO) processes, respectively. (**D–I**) Heatmaps showing clustering of genes involved in the activation or inhibition of biological pathways. (**J**) Venn diagram displaying the number of DEGs detected in CC-MII-CAPAIVM pro-cumulin compared to in CC-MII-CAPA pro-cumulin. A total of 13 DEGs from CC-MII-CAPAIVM pro-cumulin are still present in in CC-MII-CAPA pro-cumulin. Volcano plot of 49 DEGs are modulated by pro-cumulin in CC-MII-CAPA pro-cumulin. (**K**) Venn Diagram displaying the total number of transcripts detected in CCs from GV oocytes compared to CCs from MII oocytes. A total of 1852 transcripts are specific to CCs-GV, while 1127 transcripts are specific to CCs-MII. MII, metaphase II; DEGs, differentially expressed genes; CC, cumulus cells; GV, germinal vesicle; CAPA, capacitation.

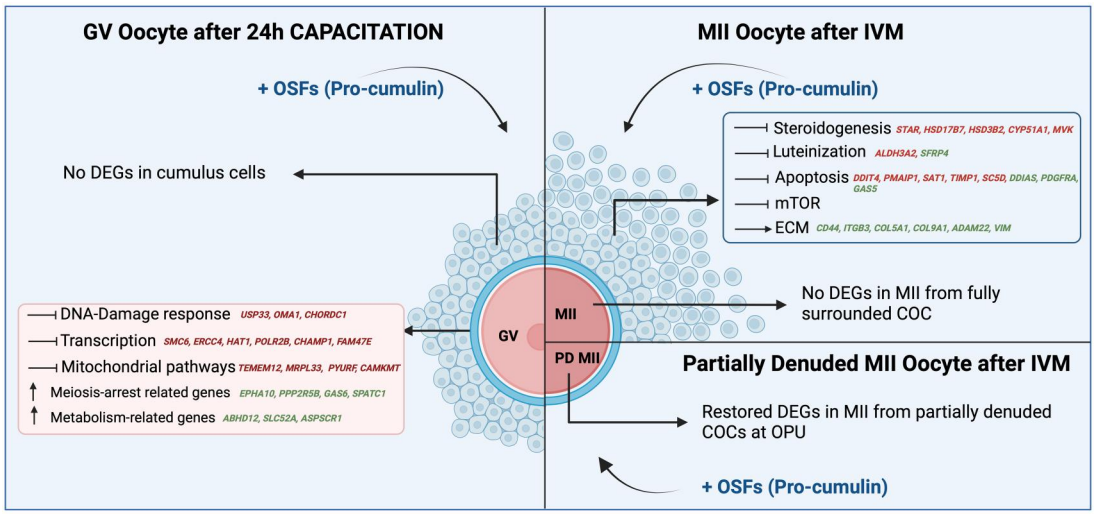

Figure 6. Overview of the impact of pro-cumulin addition in human biphasic IVM on the transcriptomes of oocytes and cumulus cells during the capacitation step (fully grown GV-stage) and maturation step (MII-stage). GV, germinal vesicle; MII, metaphase II.

stages of oocyte development. However, mature oocytes are transcriptionally silent, with accumulated mRNA being translated or stored, as the embryo relies on stored maternal transcripts and on post-transcriptional control of maternal transcripts until embryonic genome activation (Zhao *et al.*, 2020b; Hu *et al.*, 2023). Taken together, our results suggest that pro-cumulin contributes to transcription and translation silencing in cultured GV oocytes, potentially contributing to preparing the oocyte for meiosis resumption and maintaining the stability of stored maternal mRNAs. Furthermore, the lower number of expressed genes in pro-cumulin-treated compared to control GV oocytes suggests that pro-cumulin treatment promotes the degradation of transcripts as part of oocyte maturation.

Moreover, our results from the top 10 upregulated genes showed that pro-cumulin could coordinate MAPK/AKT kinases and control the meiotic arrest in fully grown GV oocytes by increasing oocyte ephrin receptor *EPHA10* and *PPP2R5B* expression to avoid a precocious nuclear maturation *in vitro* (Poliakov *et al.*, 2004). Studies have shown that ephrin receptors may negatively regulate meiosis progression, by suppressing MAPK signaling and have suggested cAMP as a transcriptional regulator of some EPH genes (Palmer and Klein, 2003; Buensuceso *et al.*, 2016). EPH signaling has also been implicated in PCOS pathology and regulation of BMP15 and GDF9 mRNA expression (Worku *et al.*, 2018; Adu-Gyamfi *et al.*, 2021). *PPP2R5B* is involved in oocyte meiosis regulation by dephosphorylating AKT1, negatively controlling cell division. Furthermore, PPP2R5B cooperates with SGO2 in protecting chromosome centromeric cohesins from separase-mediated cleavage, implicating a role in chromosome stability (Cheng and Liu, 2017). Moreover, PPP2R5B was shown to modulate the WNT signaling pathway (Liu *et al.*, 2022). Finally, genes such as *IGFBP2*, *GAS6*, *SERPINB*, with crucial roles during oocyte cytoplasmic maturation and early embryonic development were also upregulated upon pro-cumulin treatment (Sagvekar *et al.*, 2018; Spitschak and Hoeflich, 2018; Kim *et al.*, 2021). IGFBP2 is considered a biomarker for oocyte quality by enhancing mitochondrial function in oocytes (Lee *et al.*, 2023). Moreover, previous studies reported a decrease in mRNA expression of *IGFBP2* in GCs from PCOS patients (Rodríguez *et al.*, 2011).

Pro-cumulin treatment had minimal effects on the MII oocyte transcriptome for oocytes that were fully surrounded at collection. However, the transcriptomic profile of MII oocytes from partially denuded COCs cultured in CAPA-IVM differs from the fully surrounded counterparts. The bidirectional communication between oocytes and their companion somatic cells is crucial to producing competent oocytes (Gilchrist *et al.*, 2008; Russell *et al.*, 2016). During the retrieval procedure of COCs from small antral follicles in non-hCG primed IVM cycles, CCs surrounding the oocyte are more prone to mechanical disruption possibly due to the aspiration procedure. Importantly, IVM of partially denuded oocytes leads to compromised embryological outcomes in animal models (Fatehi *et al.*, 2002; Luciano *et al.*, 2005; Aguila *et al.*, 2020) and in human (unpublished data from our lab). A total of 82 DEGs were identified, which revealed alterations in lipid homeostasis, mitochondrial genes, chromatin remodeling, and methylation-related genes in MII oocytes from partially denuded COCs compared to the fully surrounded counterparts. Importantly, pro-cumulin treatment in partially denuded COCs could successfully restore the fully surrounded phenotype.

When analyzing CCs from MII oocytes after CAPA-IVM, we found that pro-cumulin had a major effect on the transcriptome, presumably by counteracting FSH-induced GC differentiation.

In vivo, mural GCs produce progesterone and oestradiol, and this phenotype differs from cumulus GCs, the somatic cells surrounding the oocyte, due to the paracrine signals mediated by OSFs (Stocco *et al.*, 2017; Turathum *et al.*, 2021; Buratini *et al.*, 2023). We have shown for the first time in human CCs after IVM, that one of the major effects of pro-cumulin in CCs is to downregulate the expression of genes involved in steroidogenesis and luteinization pathways, confirming previous findings in animal IVM models (Su *et al.*, 2004; Gilchrist *et al.*, 2008; Spicer *et al.*, 2008; Caixeta *et al.*, 2013). A recent study showed the upregulation of *SFR4* and its role in preventing luteinization when OSFs are added to a primary culture of human CCs (Esfandyari *et al.*, 2021). We corroborate this upregulated expression of *SFR4* in CCs after pro-cumulin treatment. Interestingly, the fact that pro-cumulin inactivated the mTOR pathway in CCs could be beneficial for PCOS patients, as its hyperactivation has been linked with the pathogenesis of PCOS (Liu *et al.*, 2018). Moreover, our study confirmed in human that genes involved in CC invasive migration and ECM-related genes were upregulated by OSFs, as well as genes involved in preventing apoptosis.

Different gene expression profiles in GCs have been associated with the PCOS phenotype. Metabolism pathways, insulin response genes, and ECM and cell adhesion-related genes are altered in CCs from PCOS patients (Hassani *et al.*, 2019; Sayutti *et al.*, 2022). Interestingly, in the current study, pro-cumulin could revert the upregulated gene expression of some genes associated with PCOS such as *VTN* and *HSD17B7*, suggesting that pro-cumulin may partially restore altered gene expression in CCs from PCOS.

The fact that pro-cumulin affected CC transcriptome only during the IVM step when FSH levels are high compared to the pre-IVM step suggests that pro-cumulin is a negative regulator of FSH action in CCs, promoting the CC transcriptomic profile while FSH is triggering the differentiation of the GCs into mural GCs.

In contrast to CCs from mature oocytes, CCs from GV oocytes treated with or without pro-cumulin during the capacitation step did not exhibit differences in their transcriptome profile. During the capacitation step, FSH is added in only low concentrations to enhance, together with oestradiol, CNP production to keep the oocyte under meiotic arrest. We hypothesize that this low FSH dose, compared to the IVM step, is insufficient to trigger CC dedifferentiation and hence the mitigating effects of pro-cumulin on the CC transcriptome.

In conclusion, pro-cumulin supplementation in biphasic human IVM regulates the GV oocyte transcriptome during the capacitation step promoting the expression of genes related to the fully grown GV phenotype and restoring MII transcriptome in partially denuded oocytes. Moreover, pro-cumulin upregulates genes involved in CC expansion and downregulates genes involved in apoptosis, steroidogenesis, and luteinization. Future studies should assess the effect of pro-cumulin addition in biphasic human IVM at proteomic level and embryological outcomes, assessing fertilization, the embryo epigenetic profile and aneuploidy. Furthermore, adding pro-cumulin to partially denuded COCs might potentially increase the number of *in vitro* matured competent oocytes for patients (Fig. 6).

Acknowledgements

We thank members of the Genomics Facility at Babraham for library QC and sequencing, and members of the Babraham Bioinformatics Unit for initial sequencing data processing. We thank Marius Regin for the hallmark charts and heatmaps generation.

Supplementary data

Supplementary data are available at *Molecular Human Reproduction* online.

Data availability

Datasets are available from the corresponding author upon reasonable request. Source data files for CCs, GV oocytes, and MII oocytes are provided. The dataset supporting the findings of this study is stored under restricted access in the VUB Institutional Data Repository, under the unique number (VUB/GRAD/1/000003), and the following link https://researchportal.vub.be/en/datasets/procumulin-human-transcriptome due to participant privacy concerns. Access to the data will be considered on a case-by-case basis and must be requested by contacting Prof. Ellen Anckaert (ellen.anckaert@vub.be), who will review the request. A data use agreement must be completed and signed in accordance with the VUB legal department's guidelines before any data can be shared or released. Metadata for the dataset can be accessed through the VUB Research Portal at (VUB/GRAD/1/000003). Figures 1, 2, and 6 were created with BioRender. License links: https://BioRender.com/q12p722, https://BioRender.com/v54t251 and https://BioRender.com/n20l158.

Authors' roles

B.C.-C. contributed to study design and critical discussions and performed IVM cultures, RNA-seq library generation, RNA-seq analysis, data interpretation, and manuscript drafting. A.G. contributed to RNA-seq library generation and RNA-seq analysis. H. V.R. performed IVM cultures. WS and CH were responsible for the production of pro-cumulin. J.S. was involved in the study design. M.D.V. managed the patients and supervised the clinical activities. E.A. and G.K. were involved in data interpretation, critical discussions, and manuscript revision. E.A. conceived and designed the study and was responsible for funding acquisition. All authors revised and approved the manuscript.

Funding

Work at the home institution was funded by the European Union's Horizon 2020 Research and innovation programme under the Marie Skłodowska-Curie Grant (Agreement No. 860960) and VUB Research Funding (OZR COVID extension). Work in G. K.'s lab was funded by the UK Biotechnology and Biological Sciences Research Council (BBS/E/B/000C0423), Medical Research Council (MR/S000437/1), and Wellcome Trust (210754/B/18/Z).

Conflict of interest

J.S. holds a patent on IVM (WO2016094970); and is CSO and shareholder of, and has consulting fees from, Lavima Fertility Inc. M.D.V. is the Scientific Advisory Board member of Gameto Inc and the past chair of the IVM SIG of ASRM. The remaining authors have no conflicts of interest to declare.

References

Adu-Gyamfi EA, Czika A, Liu T-H, Gorleku PN, Fondjo LA, Djankpa FT, Yu-Ding Y-B, Wang Y-Z. Ephrin and Eph receptor signaling in female reproductive physiology and pathology. *Biol Reprod* 2021; **104**:71–82.

Aguila L, Treulen F, Therrien J, Felmer R, Valdivia M, Smith LC. Oocyte selection for in vitro embryo production in bovine species: noninvasive approaches for new challenges of oocyte competence. *Animals* 2020;**10**:2196.

Akin N, Richani D, Liao X, Zhao Y, Herta AC, Billooye K, Stocker WA, Mottershead DG, Harrison CA, Smitz J et al Effect of cumulin and super-GDF9 in standard and biphasic mouse IVM. *J Assist Reprod Genet* 2022;**39**:127–140.

Angermueller C, Clark SJ, Lee HJ, Macaulay IC, Teng MJ, Hu TX, Krueger F, Smallwood SA, Ponting CP, Voet T et al Parallel single-cell sequencing links transcriptional and epigenetic heterogeneity. *Nat Methods* 2016;**13**:229–232.

Bogolyubova I, Salimov D, Bogolyubov D. Chromatin configuration in diplotene mouse and human oocytes during the period of transcriptional activity extinction. *Int J Mol Sci* 2023;**24**:11517.

Brower MA, Hai Y, Jones MR, Guo X, Chen Y-DI, Rotter JI, Krauss RM, Legro RS, Azziz R, Goodarzi MO. Bidirectional Mendelian

randomization to explore the causal relationships between body mass index and polycystic ovary syndrome. *Hum Reprod* 2019; **34**:127–136.

Buensuceso AV, Son AI, Zhou R, Paquet M, Withers BM, Deroo BJ. Ephrin-A5 is required for optimal fertility and a complete ovulatory response to gonadotropins in the female mouse. *Endocrinology* 2016;**157**:942–955.

Buratini J, Dellaqua TT, de Lima PF, Renzin MM, Canto MD, Price CA. Oocyte secreted factors control genes regulating FSH signaling and the maturation cascade in cumulus cells: the oocyte is not in a hurry. *J Assist Reprod Genet* 2023;**40**:1961–1971.

Cadenas J, la Cour Poulsen L, Mamsen LS, Andersen CY. Future potential of in vitro maturation including fertility preservation. *Fertil Steril* 2023;**119**:550–559.

Caixeta ES, Sutton-McDowall ML, Gilchrist RB, Thompson JG, Price CA, Machado MF, Lima PF, Buratini J. Bone morphogenetic protein 15 and fibroblast growth factor 10 enhance cumulus expansion, glucose uptake, and expression of genes in the ovulatory cascade during in vitro maturation of bovine cumulus-oocyte complexes. *Reproduction* 2013;**146**:27–35.

Chatroudi MH, Khalili MA, Ashourzadeh S, Anbari F, Shahedi A, Safari S. Growth differentiation factor 9 and cumulus cell supplementation in in vitro maturation culture media enhances the viability of human blastocysts. Clinical and experimental age-related loss of cohesion: causes and effects. *Int J Mol Sci* 2019; **18**:1578.

Cheng JM, Liu YX. Age-Related Loss of Cohesion: Causes and Effects. *Int J Mol Sci* 2017;**18**:1578.

De Vos M, Grynberg M, Ho TM, Yuan Y, Albertini DF, Gilchrist RB. Perspectives on the development and future of oocyte IVM in clinical practice. *J Assist Reprod Genet* 2021;**38**:1265–1280.

Diaz FJ, Wigglesworth K, Eppig JJ. Oocytes determine cumulus cell lineage in mouse ovarian follicles. *J Cell Sci* 2007;**120**:1330–1340.

Dinh DT, Breen J, Akison LK, DeMayo FJ, Brown HM, Robker RL, Russell DL. Tissue-specific progesterone receptor-chromatin binding and the regulation of progesterone-dependent gene expression. *Scientific Reports* 2019;**9**:11966.

Esfandyari S, Winston NJ, Fierro MA, Scoccia H, Stocco C. Oocyte-secreted factors strongly stimulate sFRP4 expression in human cumulus cells. *Mol Hum Reprod* 2021;**27**:gaab031.

Fatehi AN, Zeinstra EC, Kooij RV, Colenbrander B, Bevers MM. Effect of cumulus cell removal of in vitro matured bovine oocytes prior to in vitro fertilization on subsequent cleavage rate. *Theriogenology* 2002;**57**:1347–1355.

Gao M, Liu X, Du M, Gu H, Xu H, Zhong X. Identification of immune cell infiltration and effective biomarkers of polycystic ovary syndrome by bioinformatics analysis. *BMC Pregnancy Childbirth* 2023; **23**:377.

Gilchrist RB, Lane M, Thompson JG. Oocyte-secreted factors: regulators of cumulus cell function and oocyte quality. *Hum Reprod Update* 2008;**14**:159–177.

Gilchrist RB, Smitz J. Oocyte in vitro maturation: physiological basis and application to clinical practice. *Fertil Steril* 2023;**119**:524–539.

Hassani F, Oryan S, Eftekhari-Yazdi P, Bazrgar M, Moini A, Nasiri N, Sharifi-Zarchi A. Downregulation of extracellular matrix and cell adhesion molecules in cumulus cells of infertile polycystic ovary syndrome women with and without insulin resistance. *Cell J* 2019;**21**:35–42.

Hu Y, Zhang R, Zhang S, Ji Y, Zhou Q, Leng L, Meng F, Gong F, Lu G, Lin G et al Transcriptomic profiles reveal the characteristics of oocytes and cumulus cells at GV, MI, and MII in follicles before ovulation. *J Ovarian Res* 2023;**16**:225.

Hussein TS, Thompson JG, Gilchrist RB. Oocyte-secreted factors enhance oocyte developmental competence. *Dev Biol* 2006; **296**:514–521.

Khan MJ, Ullah A, Basit S. Genetic basis of polycystic ovary syndrome (PCOS): current perspectives. *Appl Clin Genet* 2019;volume**12**:249–260.

Kim K-H, Kim E-Y, Lee K-A. GAS6 ameliorates advanced age-associated meiotic defects in mouse oocytes by modulating mitochondrial function. *Aging (Albany NY)* 2021;**13**:18018–18032.

Kim K-H, Kim E-Y, Lee S-Y, Ko J-J, Lee K-A. Oocyte cytoplasmic Gas6 and heparan sulfate (HS) are required to establish the open chromatin state in nuclei during remodeling and reprogramming. *Cell Physiol Biochem* 2018;**45**:37–53.

Kõks S, Velthut A, Sarapik A, Altmäe S, Reinmaa E, Schalkwyk LC, Fernandes C, Lad HV, Soomets U, Jaakma Ü et al The differential transcriptome and ontology profiles of floating and cumulus granulosa cells in stimulated human antral follicles. *Mol Hum Reprod* 2010;**16**:229–240.

Lee D-H, Park H, You J-H, Seok J, Kwon D-W, Kim Y-R, Kim G-J. Increased IGFBP2 levels by placenta-derived mesenchymal stem cells enhance glucose metabolism in a TAA-injured rat model via AMPK signaling pathway. *Int J Mol Sci* 2023;**24**:16531.

Liu J, Wu D, Qu L, Liao H, Li M. The role of mTOR in ovarian neoplasms, polycystic ovary syndrome, and ovarian aging. *Clin Anat* 2018;**31**:891–898.

Liu J, Xiao Q, Xiao J, Niu C, Li Y, Zhang X, Zhou Z, Shu G, Yin G. Wnt/β-catenin signalling: function, biological mechanisms, and therapeutic opportunities. *Signal Transduct Target Ther* 2022;**7**:3.

Llonch S, Barragán M, Nieto P, Mallol A, Elosua-Bayes M, Lorden P, Ruiz S, Zambelli F, Heyn H, Vassena R et al Single human oocyte transcriptome analysis reveals distinct maturation stage-dependent pathways impacted by age. *Aging Cell* 2021;**20**:e13360.

Luciano AM, Franciosi F, Modina SC, Lodde V. Gap junction-mediated communications regulate chromatin remodeling during bovine oocyte growth and differentiation through cAMP-dependent mechanism(s)1. *Biol Reprod* 2011;**85**:1252–1259.

Luciano AM, Lodde V, Beretta MS, Colleoni S, Lauria A, Modina S. Developmental capability of denuded bovine oocyte in a co-culture system with intact cumulus-oocyte complexes: role of cumulus cells, cyclic adenosine 3′,5′-monophosphate, and glutathione. *Mol Reprod Dev* 2005;**71**:389–397.

Marchante M, Barrachina F, Piechota S, Fernandez-González M, Giovannini A, Smith T, Kats S, Paulsen B, González E, Calvente V et al Donor side effects experienced under minimal controlled ovarian stimulation with in vitro maturation vs. conventional controlled ovarian stimulation for in vitro fertilization treatment. *F&S Sci* 2024;**5**:242–251.

Miyara F, Migne C, Dumont-Hassan M, Meur AL, Cohen-Bacrie P, Aubriot F, Glissant A, Nathan C, Douard S, Stanovici A et al Chromatin configuration and transcriptional control in human and mouse oocytes. *Mol Reprod Dev* 2003;**64**:458–470.

Mottershead DG, Sugimura S, Al-Musawi SL, Li JJ, Richani D, White MA, Marti GA, Trotta AP, Ritter LJ, Shi J et al Cumulin, an oocyte-secreted heterodimer of the transforming growth factor-β family, is a potent activator of granulosa cells and improves oocyte quality. *J Biol Chem* 2015;**290**:24007–24020.

Nguyen DL, Nguyen NA, Pham TD, Nguyen MHN, Vuong LN. Development of children born after in vitro maturation with a prematuration step versus natural conception: a prospective cohort study. *J Assist Reprod Genet* 2022;**39**:1959–1965.

Nogueira D, Fajau-Prevot C, Clouet M, Assouline P, Deslandre M, Montagut M. Outcomes of different in vitro maturation procedures for oocyte cryopreservation for fertility preservation and yet another live birth in a cancer patient. *Life* 2023;**13**:1355.

Palmer A, Klein R. Multiple roles of ephrins in morphogenesis, neuronal networking, and brain function. *Genes Dev* 2003; **17**:1429–1450.

Pan J, Ho M. Role of glypican-1 in regulating multiple cellular signaling pathways. *Am J Physiol Cell Physiol* 2021;**321**:C846–C858.

Peng J, Li Q, Wigglesworth K, Rangarajan A, Kattamuri C, Peterson RT, Eppig JJ, Thompson TB, Matzuk MM. Growth differentiation factor 9:bone morphogenetic protein 15 heterodimers are potent regulators of ovarian functions. *Proc Natl Acad Sci USA* 2013; **110**:E776–E785.

Poliakov A, Cotrina M, Wilkinson DG. Diverse roles of Eph receptors and ephrins in the regulation of cell migration and tissue assembly. *Dev Cell* 2004;**7**:465–480.

Rodríguez FM, Salvetti NR, Panzani CG, Barbeito CG, Ortega HH, Rey F. Influence of insulin-like growth factor-binding proteins-2 and -3 in the pathogenesis of cystic ovarian disease in cattle. *Anim Reprod Sci* 2011;**128**:1–10.

Romero S, Sanchez F, Lolicato F, Van Ranst H, Smitz J. Immature oocytes from unprimed juvenile mice become a valuable source for embryo production when using C-type natriuretic peptide as essential component of culture medium. *Biol Reprod* 2016; **95**:64–64.

Russell DL, Gilchrist RB, Brown HM, Thompson JG. Bidirectional communication between cumulus cells and the oocyte: old hands and new players? *Theriogenology* 2016;**86**:62–68.

Saenz-de-Juano MD, Ivanova E, Romero S, Lolicato F, Sánchez F, Van Ranst H, Krueger F, Segonds-Pichon A, De Vos M, Andrews S et al DNA methylation and mRNA expression of imprinted genes in blastocysts derived from an improved in vitro maturation method for oocytes from small antral follicles in polycystic ovary syndrome patients. *Hum Reprod* 2019;**34**:1640–1649.

Sagvekar P, Dadachanji R, Patil K, Mukherjee S. Pathomechanisms of polycystic ovary syndrome multidimensional approaches. *Front Biosci* 2018;**10**:829.

Saucedo-Cuevas L, Ma MPQ, Le AH, Akin N, Pham TD, Ho TM, Pita G, Gonzalez-Neira A, De Vos M, Smitz J et al Epigenetic variation in neonatal tissues in infants conceived using capacitation-in vitro maturation vs. in vitro fertilization. *Fertil Steril* 2024; **121**:506–518.

Sayutti N, Abu MA, Ahmad MF. PCOS and role of cumulus gene expression in assessing oocytes quality. *Front Endocrinol (Lausanne)* 2022;**13**:843867.

Segers I, Mateizel I, Van Moer E, Smitz J, Tournaye H, Verheyen G, De Vos M. In vitro maturation (IVM) of oocytes recovered from ovariectomy specimens in the laboratory: a promising "ex vivo" method of oocyte cryopreservation resulting in the first report of an ongoing pregnancy in Europe. *J Assist Reprod Genet* 2015; **32**:1221–1231.

Spicer LJ, Aad PY, Allen DT, Mazerbourg S, Payne AH, Hsueh AJ. Growth differentiation factor 9 (GDF9) stimulates proliferation and inhibits steroidogenesis by bovine theca cells: influence of follicle size on responses to GDF91. *Biol Reprod* 2008; **78**:243–253.

Spitschak M, Hoeflich A. Potential functions of IGFBP-2 for ovarian folliculogenesis and steroidogenesis. *Front Endocrinol (Lausanne)* 2018;**9**:119.

Stocco C, Baumgarten SC, Armouti M, Fierro MA, Winston NJ, Scoccia B, Zamah AM. Genome-wide interactions between FSH and insulin-like growth factors in the regulation of human granulosa cell differentiation. *Hum Reprod* 2017;**32**:905–914.

Stocker WA, Walton KL, Richani D, Chan KL, Beilby KH, Finger BJ, Green MP, Gilchrist RB, Harrison CA. A variant of human growth differentiation factor-9 that improves oocyte developmental competence. *J Biol Chem* 2020;**295**:7981–7991.

Su Y-Q, Wu X, O'Brien MJ, Pendola FL, Denegre JN, Matzuk MM, Eppig JJ. Synergistic roles of BMP15 and GDF9 in the development and function of the oocyte-cumulus cell complex in mice: genetic evidence for an oocyte-granulosa cell regulatory loop. *Dev Biol* 2004;**276**:64–73.

Sudiman J, Ritter LJ, Feil DK, Wang X, Chan K, Mottershead DG, Robertson DM, Thompson JG, Gilchrist RB. Effects of differing oocyte-secreted factors during mouse in vitro maturation on subsequent embryo and fetal development. *J Assist Reprod Genet* 2014;**31**:295–306.

Sugimura S, Ritter LJ, Rose RD, Thompson JG, Smitz J, Mottershead DG, Gilchrist RB. Promotion of EGF receptor signaling improves the quality of low developmental competence oocytes. *Dev Biol* 2015;**403**:139–149.

Sutton-McDowall ML, Purdey M, Brown HM, Abell AD, Mottershead DG, Cetica PD, Dalvit GC, Goldys EM, Gilchrist RB, Gardner DK et al Redox and anti-oxidant state within cattle oocytes following in vitro maturation with bone morphogenetic protein 15 and follicle stimulating hormone. *Mol Reprod Dev* 2015; **82**:281–294.

Turathum B, Gao EM, Chian RC. The function of cumulus cells in oocyte growth and maturation and in subsequent ovulation and fertilization. *Cells* 2021;**10**:2292.

Virant-Klun I, Knez K, Tomazevic T, Skutella T. Gene expression profiling of human oocytes developed and matured in vivo or in vitro. *Biomed Res Int* 2013;**2013**:879489–879420.

Von Mengden L, Klamt F, Smitz J. Redox biology of human cumulus cells: basic concepts, impact on oocyte quality, and potential clinical use. *Antioxid Redox Signal* 2020;**32**:522–535.

Vuong LN, Ho VNA, Ho TM, Dang VQ, Phung TH, Giang NH, Le AH, Pham TD, Wang R, Smitz J et al In-vitro maturation of oocytes versus conventional IVF in women with infertility and a high antral follicle count: a randomized non-inferiority controlled trial. *Hum Reprod* 2020a;**35**:2537–2547.

Vuong LN, Le AH, Ho VNA, Pham TD, Sanchez F, Romero S, De Vos M, Ho TM, Gilchrist RB, Smitz J. Live births after oocyte in vitro maturation with a prematuration step in women with polycystic ovary syndrome. *J Assist Reprod Genet* 2020b; **37**:347–357.

Watson LN, Mottershead DG, Dunning KR, Robker RL, Gilchrist RB, Russell DL. Heparan sulfate proteoglycans regulate responses to oocyte paracrine signals in ovarian follicle morphogenesis. *Endocrinology* 2012;**153**:4544–4555.

Whiteley SL, Holleley CE, Wagner S, Blackburn J, Deveson IW, Marshall Graves JA, Georges A. Two transcriptionally distinct pathways drive female development in a reptile with both genetic and temperature dependent sex determination. *PLoS Genet* 2021;**17**:e1009465.

Wigglesworth K, Lee K-B, O'Brien MJ, Peng J, Matzuk MM, Eppig JJ. Bidirectional communication between oocytes and ovarian follicular somatic cells is required for meiotic arrest of mammalian oocytes. *Proc Natl Acad Sci USA* 2013;**110**:E3723–E3729.

Worku T, Wang K, Ayers D, Wu D, Ur Rehman Z, Zho H, Yang L. Regulatory roles of ephrinA5 and its novel signaling pathway in mouse primary granulosa cell apoptosis and proliferation. *Cell Cycle* 2018;**17**:892–902.

Xiong XR, Lan DL, Li J, Yin S, Xiong Y, Zi XD. Identification of differential abundances of mRNA transcript in cumulus cells and CCND1 associated with yak oocyte developmental competence. *Anim Reprod Sci* 2019;**208**:106135.

Yan H, Kolben T, Meister S, Paul C, Van Dorp J, Eren S, Kuhn C, Rahmeh M, Mahner S, Jeschke U et al Factors influencing the in vitro maturation (IVM) of human oocyte. *Biomedicines* 2021; **9**:1904.

Yeo CX, Gilchrist RB, Thompson G, Lane M. Exogenous growth differentiation factor 9 in oocyte maturation media enhances subsequent embryo development and fetal viability in mice. *Hum Reprod* 2008;**23**:67–73.

Zhang H, Vollmer M, De Geyter M, Litzistorf Y, Ladewig A, Dürrenberger M, Guggenheim R, Miny P, Holzgreve W, De Geyter C. Characterization of an immortalized human granulosa cell line (COV434). *Mol Hum Reprod* 2000;**6**:146–153.

Zhang H-L, Xu Y, Ju J-Q, Pan Z-N, Liu J-C, Sun S-C. Increased environment-related metabolism and genetic expression in the in vitro matured mouse oocytes by transcriptome analysis. *Front Cell Dev Biol* 2021;**9**:642010.

Zhang T, Zhang C, Fan X, Li R, Zhang J. Effect of C-type natriuretic peptide pretreatment on in vitro bovine oocyte maturation. *In Vitro Cell Dev Biol Anim* 2017;**53**:199–206.

Zhao Y, Liao X, Krysta AE, Bertoldo MJ, Richani D, Gilchrist RB. Capacitation IVM improves cumulus function and oocyte quality in minimally stimulated mice. *J Assist Reprod Genet* 2020a; **37**:77–88.

Zhao Z-H, Meng T-G, Li A, Schatten H, Wang Z-B, Sun Q-Y. RNA-seq transcriptome reveals different molecular responses during human and mouse oocyte maturation and fertilization. *BMC Genomics* 2020b;**21**:475.

Zheng X, Guo W, Zeng L, Zheng D, Yang S, Xu Y, Wang L, Wang R, Mol BW, Li R et al In vitro maturation without gonadotropins versus in vitro fertilization with hyperstimulation in women with polycystic ovary syndrome: a non-inferiority randomized controlled trial. *Hum Reprod* 2022;**37**:242–253.

Molecular Human Reproduction, 2025, 31, 1–15
https://doi.org/10.1093/molehr/gaaf001
Original Research